Presented at the IIR Conference,
New Applications of Natural Working Fluids
in Refrigeration and Air Conditioning
Hanover, Germany May 10-13, 1994

A SIMULATION MODEL AND STUDY OF HYDROCARBON REFRIGERANTS FOR RESIDENTIAL HEAT PUMP SYSTEMS

P.A. DOMANSKI, D.A. DIDION, W.J. MULROY, AND J. PARISE*
National Institute of Standards and Technology
Building Environment Division
Gaithersburg, MD 20899, USA

1. INTRODUCTION

To conduct a systematic study of Natural Fluids as working fluids for heat pumping applications, it was necessary for NIST to simultaneously expand its analytical tools and evaluate what design changes American industry would most readily accept. The problem was approached by categorizing all potential working fluids into one of three vapor pressure groups—high, intermediate, and low—and evaluating disadvantages presented by each category. The intermediate group spans the range covered by the CFCs that have been traditionally used (i.e., R-502 to R-11). An example of the high and low-pressure refrigerants are CO_2 and H_2O, respectively.

Both high and low-pressure refrigerants require significant hardware changes from the current designs. Acceptance of such changes depends heavily on the manufacturing costs which are difficult for anyone outside the equipment companies to determine. Informal discussions with several manufacturers of American-type heat pumps, has understandably indicated a great reluctance on their part to deviate very far from the vapor ranges traditionally used. The difficulty with the natural fluids of the intermediate-pressure range is that they are predominately flammable, and flammable fluids have virtually never been used in USA residential air-conditioning systems.

Recently, one American manufacturer made considerable effort to develop a propane heat pump. Although its performance was roughly equal to that of the traditional R-22 machines, the Underwriters Laboratory (UL) safety requirements would have increased the estimated product costs by more than 25 percent /1/. However, UL stated that these requirements would have been minimal had the flammable working fluid remained outdoors. This could be achieved by use of a secondary heat-transfer fluid, which, of course, would inflict a significant system efficiency penalty due to the increased temperature lift. The purpose of this study was to determine if this penalty can be offset by the excellent properties of hydrocarbons and glide-matching with zeotropic mixtures. Since glide-matching can be easily accomplished in the outdoor coil of an earth-coupled residential heat pump, this application was our focus. With the potential of glide matching in both the condenser and evaporator, the concept is more likely to achieve maximum thermodynamic performance.

To evaluate the concept of a new heat pump system we used a semi-theoretical model CYCLE-11 /2/, which was upgraded for the purpose of this study. It was expanded to simulate cross-flow heat exchange since the most common earth-coupled residential heat pump—used as a reference for performance evaluation—has a cross-flow air-to-refrigerant indoor coil. Also, since some hydrocarbons have considerably different transport properties than halocarbons, it was necessary to incorporate these properties into the refrigerant-side property simulations. These upgrades of CYCLE-11 are reported herein.

---

*The Pontifíca Universidade Católica, Rio de Janeiro, Brazil

2. MODELING

Background

The most efficient way for preliminary screening of different refrigerants and refrigerant mixtures is by using a semi-theoretical model of a vapor compression cycle. To fairly compare pure fluids and zeotropic mixtures, modeling at prescribed heat-sink and heat-source temperatures was proposed /3/. This paper also recommended the evaluation of different fluids at the same ratio of evaporator capacity to the sum of the evaporator and condenser heat-transfer areas. This method of modeling fairly accounts for different volumetric capacities of different refrigerants and compensates for the inevitable trade-off between capacity and the coefficient of performance (COP) when fluids are tested in the same system. With the assumption of the same overall heat-transfer coefficient in the evaporator and condenser, this ratio can be written as follows:

$$\frac{Q_e}{UA_e+UA_c} = \text{const} \qquad (1)$$

Similar results are obtained if simulations are performed at the same temperature differences between heat-transfer fluid and refrigerant in the evaporator and condenser, ΔT_e and ΔT_c. Indeed, considering that $Q_{hx}=UA_{hx}\bullet\Delta T_{hx}$, we may rearrange equation 1 as follows:

$$\frac{UA_e + UA_c}{Q_e} = \frac{1}{\Delta T_e} + \frac{Q_c}{Q_e}\frac{1}{\Delta T_c} \qquad (2)$$

Noting that Q_c/Q_e (equal to the ratio of refrigerant enthalpy change in the condenser and evaporator) does not vary significantly between different fluids, the $(UA_e+UA_c)/Q_e$ constraint is almost equivalent to ΔT model input (i.e., ΔT_e and ΔT_c are specified).

The ΔT-input simulation approach, applied in /2, 4/ can be conveniently used only for studies at a single operating condition. For multi-point evaluations this approach is inappropriate since the change in capacity with operating conditions is different for different refrigerants. This capacity change manifests itself in a refrigeration machine by establishing different ΔTs between the heat-transfer fluid and refrigerant. The UA-input approach, used in /5, 6, 7/, is preferable for multi-point simulations.

UA and ΔT CYCLE-11

The UA version of CYCLE-11 (the original ΔT version is referred to as CYCLE-11. ΔT) identifies from 5 to 11 key locations in a refrigeration system; the eleven point cycle is applicable if a four-point representation of the compressor and a liquid-line/suction-line heat exchanger are used, as shown in Figures 1 and 2. In the four-point simulation of the compressor, heat transfer and pressure drop at the suction and discharge valves (locations 1-2 and 3-4) can be accounted for by assigning heat-loss and pressure-drop parameters, as opposed to a "black box" approach where these losses can be lumped together in an overall efficiency of the compressor. The model uses original REFPROP /8/ and REFPROP-derived routines for calculating thermodynamic and transport properties of refrigerants.

CYCLE-11 simulations are performed at specified inlet and outlet temperatures of the heat-transfer fluids (HTFs) in the evaporator and condenser. In CYCLE-11.ΔT, the evaporator and condenser are represented by average effective temperature differences between the refrigerant and HTF, ΔT_e and ΔT_c, which are input data. In CYCLE-11.UA, the evaporator and condenser are represented by the product of their overall heat-transfer coefficients and heat-transfer areas, UA_e and UA_c, which are

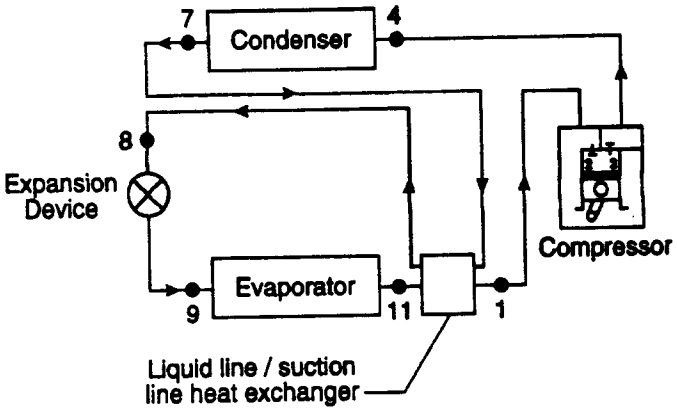

Figure 1. Schematic of a heat pump with simulated by CYCLE-11.

inputs instead of ΔT_e and ΔT_c. The input for the UA version also includes compressor RPM and displacement, while simulations by CYCLE-11.ΔT are performed for a unit mass of circulated refrigerant.

With the temperature profile for the HTFs specified, the convergence logic aims at assigning refrigerant temperatures in the condenser and evaporator so that the average temperature difference, ΔT_{hx}, between the heat exchanging fluids satisfies the basic heat-transfer relation, $Q_{hx} = UA_{hx} \cdot \Delta T_{hx}$, where UA_{hx} is the input data and Q_{hx} is the product of refrigerant mass flow rate and enthalpy change in the heat exchanger. Thus, the method for evaluating ΔT_{hx} based on the temperature profiles of HTF and refrigerant is an essential part of the model.

Average effective temperature difference

If a constant overall heat-transfer coefficient throughout the heat exchanger is assumed, the average effective temperature difference is a harmonic mean weighted with the fraction of heat transferred in individual subsections of the heat exchanger /2/:

$$\frac{1}{\Delta T_{hx}} = \frac{Q_1}{Q_{hx}\Delta T_1} + \frac{Q_2}{Q_{hx}\Delta T_2} + \ldots = \frac{1}{Q_{hx}} \sum \frac{Q_i}{\Delta T_i} \qquad (3)$$

In this equation, each term represents the contribution of each heat exchanger subsection, subsection meaning subcooled liquid, two-phase, and superheated vapor segments, or any part of the above if further division of the heat exchanger is needed to satisfy calculation requirements. Calculation of ΔT_i for an individual i^{th} subsection differs depending on the heat exchanger configuration.

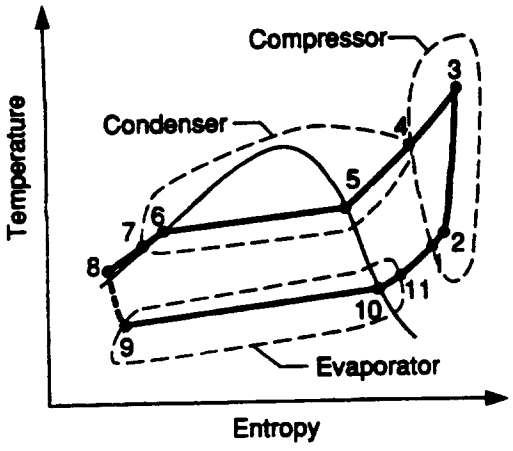

Figure 2. Temperature-entropy diagram for a heat pump working with zeotropic blend.

Counter-flow and parallel-flow. The average temperature difference for the considered subsection, ΔT_i, is evaluated by the familiar relation for the log-mean temperature difference:

$$\Delta T_i = \frac{(T_{i,out} - t_{i,in}) - (T_{i,in} - t_{i,out})}{\ln\left(\frac{T_{i,out} - t_{i,in}}{T_{i,in} - t_{i,out}}\right)} \qquad (4)$$

This equation was derived with constant specific heat and heat transfer coefficient as the primary assumptions and requires the temperature of both fluids to be known at the section inlet and outlet.

For single-component refrigerants, a heat exchanger is subdivided into three subsections according to refrigerant phase. For zeotropic mixtures, which exhibit temperature change during phase change, the two-phase section is further divided into equal enthalpy increments. This subdividing will continue up to 128 divisions until the calculated aggregate ΔT is within 0.005 K of the ΔT obtained using the previous number of subdivisions.

Cross-flow. The above relation for calculating a counter-flow ΔT_i is applicable to pure cross-flow heat transfer only if the temperature of one of the fluids stays constant. This is the case with a single-component refrigerant undergoing phase change with no pressure drop. In other cross-flow cases, the following equation is used /9/:

$$\Delta T_i = \frac{t_{i,out} - t_{i,in}}{\ln\left(\frac{r}{r + \ln(1 - rp)}\right)} \qquad (5)$$

$$\text{where} \quad r = (T_{i,in} - T_{i,out})/(t_{i,out} - t_{i,in})$$

$$p = (t_{i,out} - t_{i,in})/(T_{i,in} - t_{i,in})$$

Although the ΔT_i formulas for both counter-flow and cross-flow appear simple, the latter is much more difficult to implement in the program. For counter-flow heat exchange, the log-mean temperature equation can be easily evaluated because the inlet and outlet temperatures of the refrigerant and HTF are known for each subsection. For a cross-flow heat exchanger (approximates an air-to-refrigerant coil), the entering and leaving refrigerant temperatures and HTF entering temperature are known for each subsection. However, only the average leaving HTF temperature for the entire heat exchanger is known. The subsection outlet HTF temperature is unknown because the HTF mass flow in the subsections is unknown (since they transfer the same amount of heat instead of having the same amount of heat transfer area). Consequently, the cross-flow program must iterate until the leaving temperatures of each subsection yield the known average value for the entire heat exchanger. The successful iteration of these non-linear equations becomes increasingly more difficult as the heat exchanger temperature profile approaches a pinched condition. The iteration scheme is explained in Appendix A.

Implementation of transport properties

The UA version of CYCLE-11 was modified to include the effects of liquid transport properties. Liquid conductivity and liquid viscosity (the most influential transport properties /10/) are significantly different for R-22 and the flammable fluids of interest, as is shown in Table I. Transport properties influence cycle performance chiefly through their impact on refrigerant heat-transfer coefficient (htc) and pressure drop in heat exchangers. Because of its semi-theoretical design, CYCLE-11.UA does not take detailed heat exchanger data as input, and detailed modeling of the evaporator and condenser is not possible. However, it is possible to include a simplified representation of transport properties on a relative basis using the performance of a reference fluid as a reference.

Table I. Selected Properties of Studied Refrigerants at Standard Atmospheric Pressure

Refrigerant	Weight Composition	Molecular Weight	Dew-Point Temperature	Temperature Glide[1]	Vapor[2] Molar Heat Capacity	Liquid Thermal Conductivity	Liquid Absolute Viscosity
	(%)	(g/mol)	(°C)	(°C)	(j/mol°C)	(W/m°C)	(micropoise)
R-22	100	86.47	-40.8	0	50.37	0.1286	3369
R-290	100	44.10	-42.1	0	63.05	0.1523	1999
R-290/600a	70/30	47.54	-30.8	6.7	69.60	0.1448	2171
R-32/152a	49/51	58.34	-35.3	8.1	48.85	0.1798	3039

(1) - dew point minus bubble point (2) - saturated state at atmospheric pressure

Heat-transfer coefficient. The total resistance to heat transfer in a heat exchanger can be represented as a summation of the resistance on the refrigerant side and the combined resistance of the heat exchanger material and the resistance on the heat-transfer-fluid side:

$$\frac{1}{UA_{hx}} = R_{hx} = R_r + R^* \tag{6}$$

$$\text{where } R^* = R_{tube} + R_{HTF} \tag{7}$$

Consequently, we may write:

$$R^* = \frac{1}{UA_{hx}}\left(1 - \frac{UA_{hx}}{h_r A_r}\right) \tag{8}$$

Resistance R^* is independent of refrigerant, and is assumed to be independent of operating conditions. The value of R^* is evaluated by conducting a reference simulation (for the reference refrigerant and operating conditions) using values for A_r and UA_{hx} as input data. The inside-tube htc, h_r, is then calculated for the actual refrigerant conditions. The value of R^* is stored in a data file, and is used in subsequent simulations (at different operating conditions or for a different refrigerant) to calculate the overall conductance by the following equation:

$$UA_{hx} = \frac{1}{R^* + \frac{1}{h_r A_r}} \tag{9}$$

The refrigerant-side heat-transfer coefficient is calculated using correlations developed for smooth tubes. For evaluating the evaporation heat-transfer coefficient, the program uses the forced-convection term of the correlation for binary mixtures developed by Jung /11/:

$$h_{conv} = C_{me} \cdot F_p \cdot h_{lo} \tag{10}$$

$$\text{where } C_{me} = 1 - 0.35\,[ABS(Y-X)]^{1.56}$$

$$h_{lo} = 0.023\,\frac{k_l}{d}\left(\frac{G(1-x)d}{\mu_l}\right)^{0.8}\left(\frac{c_{pl}\mu_l}{k_l}\right)^{0.4}$$

$$F_p = 2.37(0.29 + \frac{1}{X_{tt}})^{0.85} \quad (11)$$

Coefficient C_{mc} is a penalty factor to account for the mass diffusion that occurs when evaporating refrigerant mixtures. The nucleate-boiling term of Jung's correlation is omitted here because it requires surface-tension data which are not available for all 38 fluids covered by CYCLE-11. This omission is justified because it is seldom significant for in-tube evaporator.

The condensation heat-transfer coefficient is calculated by the well-known correlation of Traviss et al. /12/. Although developed for pure fluids, this correlation placed 85 percent of its predictions within 20 percent of the experimental values for pure fluids and mixtures reported in /13/.

Evaporation and condensation heat-transfer coefficients used by CYCLE-11.UA are averages of the values calculated for four equally-spaced points (on the enthalpy scale) within the two-phase regime. To account for the sensitivity of heat-transfer coefficients to refrigerant mass flow, the program determines the number of circuits in the heat exchanger for the reference simulation based on a prescribed tube diameter and refrigerant mass flux. This definition of coil circuitry is used during the subsequent runs, which may have a different refrigerant mass flow rate resulting in a different mass flux.

Pressure drop. Similar to heat transfer, pressure drop simulations are performed on a relative basis to a simulated case for the reference simulation. Pressure drop in the evaporator is simulated using the frictional term of the Pierre correlation /14/. This term can be rearranged to the following form:

$$\Delta P = DP_e \cdot m_r^{1.75} v_{v,m} [(i_{10} - i_9)\mu_l]^{0.25} \quad (12)$$

where DP_e combines the effects of the tube length, tube diameter, and a numerical constant of the Pierre correlation. For a given evaporator DP_e is a constant and is evaluated for a reference simulation at which the pressure drop is specified. It is then used for estimating the pressure drop in this heat exchanger in subsequent simulations which may be conducted with a different refrigerant or set of operating conditions.

The pressure drop in the condenser is simulated using the Lockhart-Martinelli method /15/ which relates two-phase and single-phase pressure gradient:

$$\left(\frac{dP}{dz}\right)_{tph} = \phi_v^2 \left(\frac{dP}{dz}\right)_v \quad (13)$$

with the following approximation of Φ_v /16/:

$$\Phi_v = 1 + 2.85X_{tt}^{0.523} \quad (14)$$

Again, combining the tube length and diameter effects with a numerical constant, the following relation is obtained for a given refrigerant flow quality:

$$\left(\frac{dP}{dz}\right)_{tph} = DP_c \, \Phi_v^2 \, m_r^{1.8} \, v_v \, \mu_v^{0.2} \quad (15)$$

where DP_c is a refrigerant-independent constant for a given condenser. The value of the DP_c parameter is calculated for the reference run with a specified pressure drop. A single mid-enthalpy point between saturated vapor and liquid is used for pressure drop calculations.

Verification

The program was verified by comparing its predictions to laboratory measurements for the refrigerants R-290 and R-134a/600a presented in /17/. Verification was conducted by using the laboratory data for R-22 as the reference case. Simulation of the other refrigerants was then performed without additional experimental input. Without the transport property option, the program underpredicted both the capacity and COP for R-290 by 2.5 percent. With the inclusion of transport properties, the capacity and COP for R-290 were predicted within 0.6 percent.

For the mixture R-134a/600a, the capacity and COP were overpredicted by 3.9 percent and 13.4 percent, respectively, when transport properties were not used. With the transport properties, the capacity and COP were overpredicted by 4.9 percent and 14.4 percent, respectively. To identify the reason for this disparity, the experimental data for R-22 and R-134a/600a were examined. It was found that the compressor efficiency was degraded in tests with the mixture.

The compressor efficiency is provided as input to CYCLE-11 and is not recalculated for different refrigerants. Other experimental work /18, 19/ has shown reciprocating compressor efficiency to degrade with decreasing volumetric capacity refrigerants, and the results of /17/ are consistent with such observations in that the experimental capacity measurements for R-290 and R-134a/600a were 90 percent and 70 percent of R-22 respectively. This efficiency degradation may be attributed the capacity decreasing while mechanical losses remain constant.

3. SYSTEM EVALUATION

System Concept

To implement the Lorenz cycle system, counter-flow heat exchangers for the evaporator and condenser are required. This makes it possible to match the temperature glide between the phase-changing refrigerant and the secondary heat-transfer fluid. If the HTF is a liquid many off-the-shelf heat exchangers, both tube-in-tube and plate, are available. Figure 3 represents one possible scheme in which such a concept might be implemented. The refrigerant system is a simple one-way circuit which can be hermetically sealed at the factory. The heating/cooling mode reversal is established in the secondary heat-transfer fluid side with the addition of two reversing valves and pumps. The indoor coil system may consist of one central coil with an air duct distribution system or perhaps a plastic-pipe system with a water coil for each room. The outdoor coil would be buried in the earth for year-round moderate temperature exposure. This system would be intended to replace the current US earth-coupled heat pump system shown in Figure 4. In this system, the complexity of reversing heating modes is transferred from the refrigerant side to the water side.

Simulation Results

Tables II through VII present simulation results for three systems without and with liquid-line/suction-line heat exchange (LSHX). The systems modeled in these tables (shown in Figure 3) differs from conventional water-to-air residential systems in the isolation of the refrigerant in the outdoor unit, a necessity for flammable refrigerants. Isolation of the refrigerant is achieved by employing an additional water loop to transfer heat to or from the indoor coil.

The three simulated water-to-water heat pumps differ by the size of the water-to-refrigerant heat exchangers. The heat exchanger size is represented by the refrigerant-to-water ΔT. Since the reference case for this study is the conventional earth-coupled water-to-air heat pump, the heat exchangers for the water-to-water heat pumps were sized with reference to the conventional system. The ΔT listed in the tables is for the refrigerant-to-water heat exchanger for a corresponding conventional heat pump operating in the cooling mode. The same size water-to-refrigerant heat

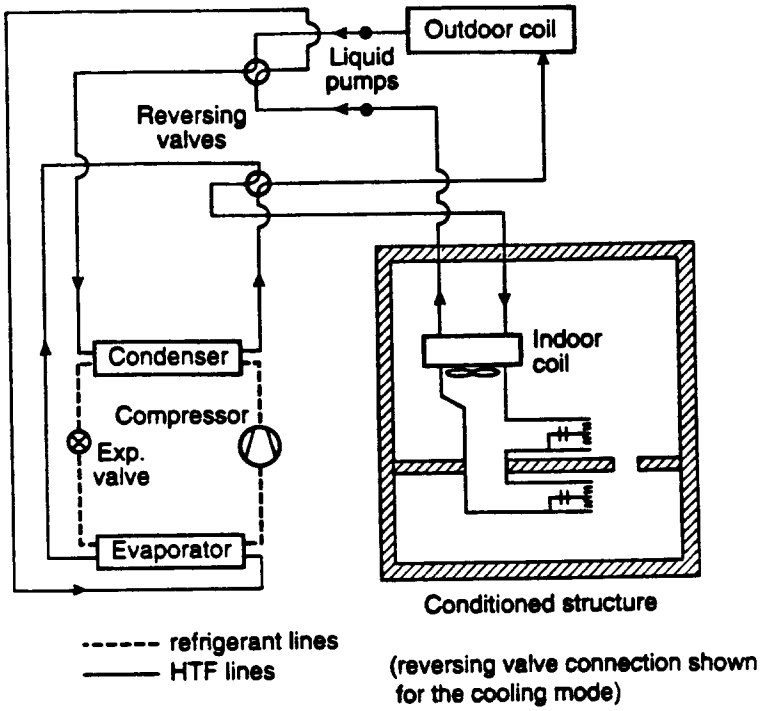

Figure 3. Schematic of NIST water-to-water heat pump.

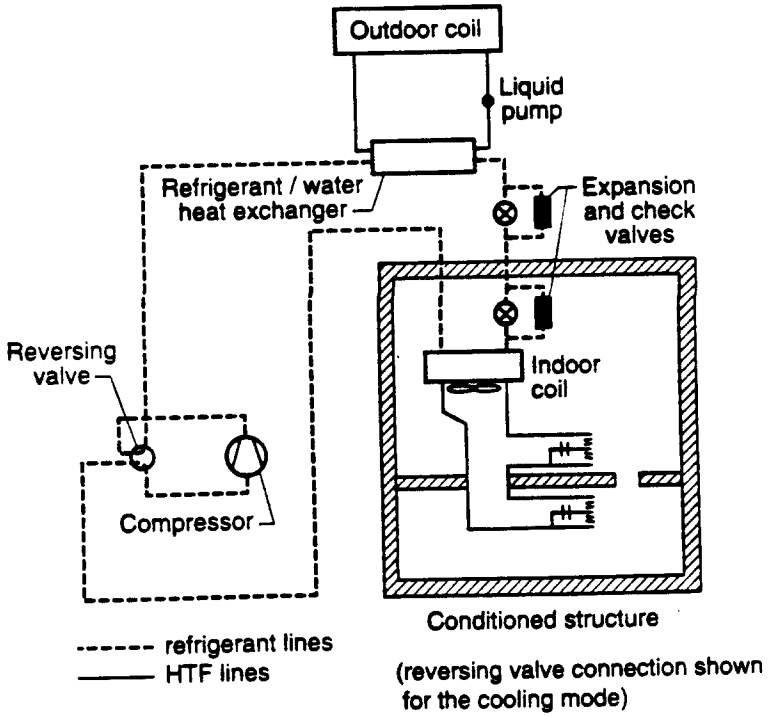

Figure 4. Schematic of water-to-air, earth-coupled heat pump.

exchanger was used by the water-to-water system in the indoor water loop. In the cooling mode, the water inlet and outlet temperatures to the evaporator and condenser were 13°C and 7°C, and 29°C and 35°C, respectively. In the heating mode, these temperatures were 5°C and 1°C, and 39°C and 45°C. Condenser subcooling and evaporator superheat were zero. All simulations were performed for a reciprocating hermetic compressor with an electric-motor efficiency of 0.9 and polytropic efficiency of 0.7

The comparison base, which was used as a divisor for normalizing the values in Tables II through VII, was a conventional water-to-air, earth-coupled R-22 heat pump. This comparison base, shown as the first entry in Table II, is representative of current, high efficiency, conventional, water-to-air systems. The first entry in Tables III through VII similarly labeled "R-22, water-to-air" shows the effect of increased heat exchanger size or addition of liquid-line/suction-line heat exchange on the comparison base system. This provides another comparison where the base system would have the same benefit of the increased heat exchanger surfaces that the proposed NIST system requires. The next entry in these tables for R-22 in the water-to-water cycle is indicative of the efficiency loss as a result of the heat exchange to an extra indoor water loop. The remaining entries are for R-290 (propane), R-290/600a (propane/isobutane) mixture, and a mixture of R-32/152a, all of which were simulated in the water-to-water system. All selected R-22 alternatives are flammable, but R-290 and R-290/600a are environmentally preferable over R-32/152a. The R-32/152a mixture was included in this study because it is one of the best non-CFC halogenated zeotropes against which the performance of hydrocarbons may be gauged.

The two zeotropic mixtures, R-290/600a and R-32/152a, were felt to be particularly appropriate for this water-to-water cycle because of the possibility of efficiency improvement by glide matching. The composition for R-290/600a, 70 percent R-290, was arbitrarily chosen as a tradeoff of slightly increased efficiency versus greatly reduced capacity. The performance of mixtures of R-290/600a with more than 70 percent R-290 would be expected to be intermediate in performance to the endpoint refrigerants.

Simulations were performed with the cooling mode capacity kept constant at the base cycle value for Table II. This was accomplished by varying compressor volumetric capacity listed as "Relative Comp. Size" in Tables II through VII except for the R-32/152a mixture, which compositions R-32/152a were chosen to give the same cooling capacity as the base case R-22 cycle. This was possible since R-32 has a greater and R-152a less capacity than R-22. Different R-32 concentrations were used for the different Tables II through VII since capacity degradation from the base cycle varied as a result of the various assumptions used in generating these tables.

Compressor size was kept constant between heating and cooling. Use of a larger compressor to compensate for reduced cooling capacity (resulting from lowering of the evaporating temperature and suction gas density with introduction of the indoor water loop) resulted in increased capacity in heating because the indoor water loop was now on the condenser side and had less effect on capacity.

Table II presents results for the proposed water-to-water heat pump which corresponds to a current, high-efficiency, residential water-to-air system. No liquid-line/suction-line heat exchanger is employed and the refrigerant-to-water heat exchangers are sized as in a higher efficiency unit (5°C average temperature difference between the refrigerant and the indoor water loop; a 7.5°C ΔT would be typical for an average efficiency unit and a 10°C ΔT for a low efficiency unit). Cooling efficiencies range from 80 percent to 86 percent of the R-22 base case cycle. Because of secondary greenhouse warming effects these efficiencies are too low to be acceptable, particularly since it will be shown that improvement to comparability with the R-22 base case can be obtained.

In Table III, LSHX with a 5°C approach temperature was added and the indoor loop heat exchanger temperature difference was kept at 5°C. The hydrocarbon refrigerants benefited more than the

R-32/152a mixture from LSHX because of their larger molar heat capacity. The highest tabulated cooling efficiency, 88 percent of the R-22 base case, is still undesirably low.

Table IV presents performance without LSHX but with the heat exchangers doubled in size which resulted in the reduction of the refrigerant-to-water temperature difference from 5°C to 2.5°C in the corresponding water-to-air system. As would be expected, this change is most beneficial to the zeotropic mixtures which can now proportionally benefit more from glide matching. The highest alternative fluid efficiency is now exhibited by the R-32/152a mixture, 103 percent of the base case cycle efficiency in cooling and 100 percent in heating.

In Table V, LSHX is added to the system of Table IV. As in Table III, addition of LSHX provides significant additional benefit only to the large molecule (i.e., greater c_p) hydrocarbon refrigerants. For this case all three substitute refrigerants provide efficiency comparable to or superior to the R-22 base case but somewhat lower than R-22 in a water-to-air system with equivalently sized heat exchangers.

Table VI presents the performance of a system without LSHX and with the heat exchangers doubled in size from the Table IV values. The doubling of the heat exchanger size reduced the refrigerant-to-water temperature difference from 2.5°C to 1.25°C in the corresponding water-to-air system. This change is most beneficial to the zeotropic mixtures which are capable of glide matching, while the

Table II: Simulated comparison of a water-to-water, earth-coupled, heat pump with a 5°C ΔT across the refrigerant-to-water heat exchangers to a conventional, water-to-air, earth-coupled, R-22 heat pump.

	Relative	Cooling Mode		Heating Mode	
	Comp. Size	Q	COP	Q	COP
R-22,water-to-air	1.00	1.00	1.00	1.00	1.00
R-22	1.20	1.00	0.80	1.18	0.90
R-290	1.42	1.00	0.80	1.16	0.90
R-290/600a(70/30)	1.72	1.00	0.84	1.12	0.92
R-32/152a(59/41)	1.00	1.00	0.86	1.15	0.93

Table III: Simulated comparison of a water-to-water, earth-coupled, heat pump with a 5°C ΔT across the refrigerant-to-water heat exchangers and with liquid-line/suction-line heat exchange to a conventional, water-to-air, earth-coupled, R-22 heat pump.

	Relative	Cooling Mode		Heating Mode	
	Comp. Size	Q	COP	Q	COP
R-22,water-to-air	1.01	1.00	1.01	1.01	1.04
R-22	1.21	1.00	0.81	1.19	0.92
R-290	1.37	1.00	0.84	1.19	0.95
R-290/600a(70/30)	1.65	1.00	0.88	1.16	0.98
R-32/152a(60/40)	1.00	1.00	0.86	1.15	0.93

pure refrigerants are now pinched. Consequently the two zeotropes now more than compensate for the efficiency loss caused by adding the indoor water loop, matching or slightly outperforming R-22 in the conventional water-to-air system.

Table IV: Simulated comparison of a water-to-water, earth-coupled, heat pump with a 2.5°C ΔT across the refrigerant-to-water heat exchangers to a conventional, water-to-air, earth-coupled, R-22 heat pump.

	Relative	Cooling Mode		Heating Mode	
	Comp. Size	Q	COP	Q	COP
R-22,water-to-air	0.98	1.00	1.09	1.00	1.02
R-22	1.12	1.00	0.92	1.14	0.95
R-290	1.32	1.00	0.91	1.12	0.95
R-290/600a(70/30)	1.54	1.00	1.01	1.08	1.00
R-32/152a(49/51)	1.00	1.00	1.03	1.09	1.00

Table V: Simulated comparison of a water-to-water, earth-coupled, heat pump with a 2.5°C ΔT across the refrigerant-to-water heat exchangers and with liquid-line/suction-line heat exchange to a conventional, water-to-air, earth-coupled, R-22 heat pump.

	Relative	Cooling Mode		Heating Mode	
	Comp. Size	Q	COP	Q	COP
R-22,water-to-air	0.99	1.00	1.09	1.02	1.06
R-22	1.13	1.00	0.92	1.16	0.96
R-290	1.28	1.00	0.96	1.15	1.00
R-290/600a(70/30)	1.50	1.00	1.05	1.11	1.06
R-32/152a(50/50)	1.00	1.00	1.03	1.10	1.00

Table VI: Simulated comparison of a water-to-water, earth-coupled, heat pump with a 1.25°C ΔT across the refrigerant-to-water heat exchangers to a conventional, water-to-air, earth-coupled, R-22 heat pump.

	Relative	Cooling Mode		Heating Mode	
	Comp. Size	Q	COP	Q	COP
R-22,water-to-air	0.97	1.00	1.12	1.00	1.02
R-22	1.10	1.00	0.96	1.13	0.96
R-290	1.30	1.00	0.95	1.10	0.95
R-290/600a(70/30)	1.47	1.00	1.11	1.06	1.04
R-32/152a(44/56)	1.00	1.00	1.13	1.06	1.04

Table VII presents performance with LSHX and with the heat exchangers sized at the Table VI values. As would be expected, the R-22 and R-32/152a efficiency is little changed from the Table VI values whereas the hydrocarbon refrigerants show an efficiency improvement of approximately 3 percent from their Table VI values.

Although not listed in Tables II through VII, compressor discharge temperatures and pressures for the most likely to be applied configurations are worthy of comment. For R-290 and R-290/600a this would be the configuration of Table VII. For this configuration the predicted discharge temperature and pressure for R -290 are 5.5°C above and 234 kPa below the base-case, no-LSHX, R-22 values in cooling, and 16.2°C above and 97 kPa below in heating. The predicted discharge temperature and pressure for the R-290/600a mixture are 3.4°C below and 500 kPa below the base-case, no-LSHX, R-22 values in cooling, and 6.4°C above and 419 kPa below in heating.

Since the mixture R-32/152a showed little benefit from LSHX, the most likely to be applied configuration for this mixture would be that of Table VI. For this configuration the predicted discharge temperature and pressure for R-32/152a are 1.5°C above and 162 kPa below the base-case, no-LSHX, R-22 values in cooling, and 9.1°C above and 39 kPa above in heating.

Table VII: Simulated comparison of a water-to-water, earth-coupled, heat pump with a 1.25°C ΔT across the refrigerant-to-water heat exchangers and with liquid-line/suction-line heat exchange to a conventional, water-to-air, earth-coupled, R-22 heat pump.

	Relative	Cooling Mode		Heating Mode	
	Comp. Size	Q	COP	Q	COP
R-22,water-to-air	0.99	1.00	1.12	1.02	1.06
R-22	1.11	1.00	0.95	1.13	0.97
R-290	1.26	1.00	0.98	1.13	1.00
R-290/600a(70/30)	1.44	1.00	1.14	1.09	1.09
R-32/152a(45/55)	1.00	1.00	1.12	1.06	1.03

4. CONCLUDING REMARKS

The three fluids examined in a water-to-water loop heat pump are viable alternatives to R-22 in a conventional ground water heat pump, but each has its tradeoffs. R-290 and its mixtures require a larger compressor. R-32/152a has the disadvantage of being a man-made chemical with some GWP. The predicted performance levels are sufficiently close to the R-22 base case cycle to be commercially viable at this time. Hence, further investigation into system design and refrigerant selection for heat pumps using flammable, environmentally-benign fluids isolated outside the habitable envelope is well justified.

5. ACKNOWLEDGEMENTS

The authors appreciate the support of the National Institute of Standards and Technology and the Electronic Power Research Institute under Project Number RP 3412-54, Mr. Terry Statt, Project Manager. Also, Dr. Parise's sabbatical at NIST was made possible through the support of the Ministries for Education and for Science and Technology of the Brazilian Government.

6. REFERENCES

1. Treadwell, D., (Lennox Ind.) "Packaged Air Conditioning Equipment Employing Propane", (oral presentation only) ARI Flammability Workshop, Chicago, IL, March 8-9, 1994.
2. Domanski, P.A., McLinden, M.O., "A Simplified Cycle Simulation Model for the Performance Rating of Refrigerants and Refrigerant Mixtures", Int. J. Refrig., Vol 15, No. 2, pp. 81-88, (1992).
3. McLinden, M., and Radermacher, R., "Methods for Comparing the Performance of Pure and Mixed Refrigerants in the Vapor Compression Cycle", Int. J. Refrig., Vol. 10, pp. 318-325, (1985).
4. Rice, C.K., Sand, R.J., "Initial Parametric Results Using CYCLEZ—An LMTD-Specified Lorenz-Meutzner Cycle Refrigerator-Freezer Model", Proceedings of the 1990 ASHRAE-Purdue CFC Conference, Purdue University, West Lafayette, Indiana, USA.
5. Domanski, P.A., Didion, D.A., "Thermodynamic Evaluation of R-22 Alternative Refrigerants and Refrigerant Mixtures", ASHRAE Transactions, Vol. 99, Pt. 2, (1993).
6. Radermacher, R., Jung, D.S., "Theoretical Analysis of Replacement Refrigerants for R22 for Residential Usage", ASHRAE Transactions, Vol. 99, Pt. 1, (1993).
7. Hogberg, M., Vamling, L., Berntsson, T., "Calculation methods for comparing the performance of pure and mixed working fluids in heat pump application", Int. J. Refrig., Vol. 16, No. 6, pp. 403-413, (1993).
8. Gallager, J., McLinden, M.O., Morrison, O., Huber, M.,"NIST Standard Reference Data Base 23, Version 4.0" (REFPROP), National Institute of Standards and Technology, Gaithersburg, MD, USA, (1993).
9. Threlkeld, J.L., "Thermal Environmental Engineering", Prentice-Hall, Inc., Englewood Cliffs, NJ, (1970).
10. Domanski, P.A., Didion, D.A., "Impact of Refrigerant Property Uncertainties on Prediction of Vapor Compression Cycle Performance", NBSIR 86-3373, National Bureau of Standards, Gaithersburg, MD, USA, (1986).
11. Jung, D.S., "Horizontal-Flow Boiling Heat Transfer Using Refrigerant Mixtures", Report ER-6364, Electric Power Research Institute, Palo Alto, CA, USA, (1989).
12. Traviss, D.P., Rohsenow, W.M., Baron, A.B., "Forced-Convection Condensation Inside Tubes: A Heat Transfer Equation for Condenser Design", ASHRAE Transactions, Vol. 79, Part 1, pp. 157-165, (1973).
13. DeGrush, D., Stoecker, W.F., "Measurements of Heat-Transfer Coefficients of Nonazeotropic Refrigerant Mixtures Condensing Inside Horizontal Tubes", ORNL/Sub/81-7762/6/ & 01, Oak Ridge National Laboratory, Oak Ridge, TN, USA, (1987).
14. Pierre, B., "Stromningsmotstand vid Kikande Koldmedier", Kylteknisk Tidskrift, No. 6, (1957).
15. Lockhart, R.W., Martinelli, R.C., "Proposed Correlation of Data for Isothermal Two-Phase, Two-Component Flow in Pipes", Chemical Engineering Progress, Vol. 45, pp. 39-48, (1949).
16. Soliman, M., Schuster, J.R., Berenson, P.J., "A General Heat Transfer Correlation for Annular Flow Condensation", Journal of Heat Transfer, Vol. 90, pp. 267-76, (1968).
17. Kim, M.S., Mulroy, W.J., Didion, D.A., "An Experimental Evaluation of the Flammability and Performance Potentials of Two Azeotropic Refrigerant Mixtures", Presented at the 6th International Symposium on Transport Phenomena (ISTP-6) in Thermal Engineering, Seoul, Korea, (1993).
18. Buschmeier, M., Mulroy, W., Didion, D., "An Initial Laboratory Evaluation of a Single Solution Circuit Cycle for use with Nonazeotropic Refrigerants", NISTIR 4406, National Institute of Standards and Technology, Gaithersburg, MD, USA, (1990).
19. Stoecker, W., McCarthy, C., "The Simulation and Performance of a System Using an R12/R114 Refrigerant Mixture", ORNL/Sub/81-7762/3&01, Oak Ridge National Laboratory, Oak Ridge, TN, USA, (1981).

20. Domanski, P., Didion, D., Doyle, J., "Evaluation of Suction Line-Liquid Line heat Exchange in the Refrigeration Cycle", IIR Conference, Purdue, July 14-17, 1994.

NOMENCLATURE

A - area
G - refrigerant mass flux
HTF - heat transfer fluid
P - pressure
Q - capacity
R - heat-transfer resistance
T - temperature of refrigerant
U - heat-transfer conductance
X - liquid-phase molar composition
Y - vapor-phase molar composition
X_{tt} - Lockhart-Martinelli parameter
c_p - heat capacity
d - tube inside diameter
h - heat transfer coefficient
i - enthalpy
k - thermal conductivity
m - mass flow rate
t - temperature of HTF
v - specific volume
x - flow quality
z - length
μ - absolute viscosity

Subscripts:
c - condenser
e - evaporator
hx - heat exchanger
l - liquid
m - mean value
r - refrigerant
tph - two phase
v - vapor

APPENDIX A. Iteration procedure for calculating the average effective temperature difference for a pure cross-flow heat exchanger

The input data to this procedure includes the total heat-transfer rate (Q_{hx})in the heat exchanger, overall heat-transfer conductance (UA_{hx}), HTF temperatures and thermodynamic state of refrigerant at the heat exchanger inlet and outlet. To evaluate of the average effective temperature difference between HTF and refrigerant, ΔT_{hx}, the heat exchanger is divided into subsections for which individual ΔT_i are calculated and are used to obtain ΔT_{hx} by equation (3). The number of subsections is such that doubling the number of subsections does not change the value of calculated ΔT_{hx} by more than 0.005K.

To explain the procedure, let's consider an individual i^{th} subsection in the condenser. The division of the heat exchanger into subsections is performed on the enthalpy scale. Thus, the heat transfer rate in the section, Q_i, and inlet and outlet parameters of refrigerant (including temperatures) are known. Also known is the inlet temperature of the HTF, but the outlet HTF temperature for this subsection is unknown. Instead, the HTF temperature leaving the condenser is available (input datum).

At the outset of iteration, the fraction of the total heat exchanger overall conductance used in this subsection, $F_i = UA_i/UA_{hx}$, has to be assumed. F_i is also equal to the fraction of the total flow rate of the HTF used in the section. As the first guess, $F_i = Q_i/Q_{hx}$. Then the following steps are used.

1. Calculate the thermal capacitance of the heat transfer fluid for the entire heat exchanger.

$$m_{hx} \cdot c_p = Q_{hx}/(t_{out} - t_{in}) \quad \text{(A1)}$$

2. Calculate the thermal capacitance and leaving temperature ($t_{i,out}$) of HTF in the i^{th} subsection.

$$m_i \cdot c_p = F_i \cdot m_{hx} \cdot c_p \quad \text{(A2)}$$

$$t_{i,out} = t_{in} + Q_i/(m_i \cdot c_p) \quad \text{(A3)}$$

3. Calculate the average temperature difference, ΔT_i, between the refrigerant and the heat transfer fluid for the i^{th} subsection using equation 5.

4. Calculate UA for the i^{th} subsection.

$$UA_i = Q_i/\Delta T_i \quad \text{(A4)}$$

Steps 1 through 4 are performed for all subsection. Then calculation procedure advances to step 5.

5. Check the convergence.

$$UA_{hx} = \sum UA_i \quad \text{(A5)}$$

$$F_i' = UA_i/UA_{hx} \quad \text{(A6)}$$

If $F_i' \neq F_i$, estimate new F_i and go to step 1,
otherwise calculate the average effective temperature difference for the heat exchanger.

$$\Delta T_{hx} = \frac{Q_{hx}}{\sum \frac{Q_i}{\Delta T_i}} \quad \text{(A7)}$$

This ΔT_{hx} value is then compared to the ΔT_{hx} value obtained from the previous iteration loop. If the two values are not within the prescribed tolerance (0.005K), the heat exchanger is further subdivided (each subsection split by half) and calculations are repeated.

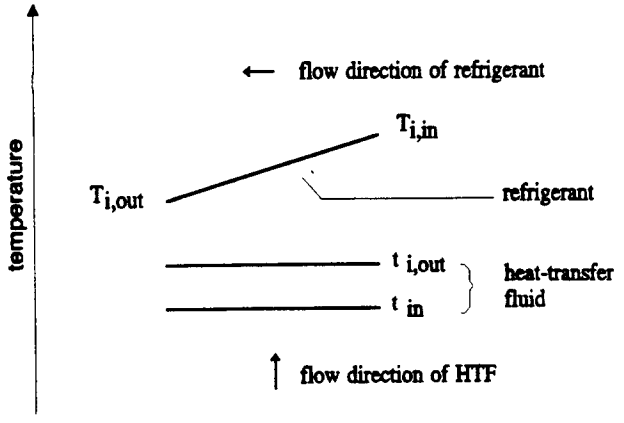

Figure A1. A schematic representation of fluids temperature in the i^{th} subsection of a cross-flow heat exchanger.

ABSTRACT

The paper presents exploratory evaluation of a new concept of residential heat pump which facilitates the application of flammable refrigerants. The evaluation was performed using an improved version of semi-theoretical vapor compression cycle model (CYCLE-11), which is also described. This improved version allows for counter, cross, and parallel-flow heat exchangers, and can account for differences in transport properties of working fluids. The latest NIST refrigerant properties algorithm (REFPROP4) has been incorporated providing 38 different refrigerants with up to five components mixture capabilities.

The new heat pump concept is a derivative of an earth-coupled heat pump with a heat-transfer fluid circulating indoors, thus keeping the flammable refrigerant outside. Performance of R-290, R-290/600a, R-22, and R-32/152a was simulated. The benefits of glide matching and better fluid properties are shown to substantially offset the performance deficits due to using secondary fluid loops needed to maintain the outdoor isolation of the flammable refrigerants.